The Plant Cell, Vol. 26: 1512–1524, April 2014, www.plantcell.org

The Rice Basic Helix-Loop-Helix Transcription Factor TDR INTERACTING PROTEIN2 Is a Central Switch in Early Anther Development[C][W]

Zhenzhen Fu,[a] Jing Yu,[a] Xiaowei Cheng,[b] Xu Zong,[b] Jie Xu,[a] Mingjiao Chen,[a] Zongyun Li,[b] Dabing Zhang,[a] and Wanqi Liang[a,1]

[a] State Key Laboratory of Hybrid Rice, School of Life Sciences and Biotechnology, Shanghai Jiao Tong University, Shanghai 200240, China
[b] School of Life Science, Jiangsu Normal University, Xuzhou, Jiangsu 221116, China

In male reproductive development in plants, meristemoid precursor cells possessing transient, stem cell–like features undergo cell divisions and differentiation to produce the anther, the male reproductive organ. The anther contains centrally positioned microsporocytes surrounded by four distinct layers of wall: the epidermis, endothecium, middle layer, and tapetum. Here, we report that the rice (*Oryza sativa*) basic helix-loop-helix (bHLH) protein TDR INTERACTING PROTEIN2 (TIP2) functions as a crucial switch in the meristemoid transition and differentiation during early anther development. The *tip2* mutants display undifferentiated inner three anther wall layers and abort tapetal programmed cell death, causing complete male sterility. TIP2 has two paralogs in rice, TDR and EAT1, which are key regulators of tapetal programmed cell death. We revealed that TIP2 acts upstream of TDR and EAT1 and directly regulates the expression of *TDR* and *EAT1*. In addition, TIP2 can interact with TDR, indicating a role of TIP2 in later anther development. Our findings suggest that the bHLH proteins TIP2, TDR, and EAT1 play a central role in regulating differentiation, morphogenesis, and degradation of anther somatic cell layers, highlighting the role of paralogous bHLH proteins in regulating distinct steps of plant cell–type determination.

INTRODUCTION

The formation of organized and functional organs requires the establishment of new cell lineages. Within the dominant diploid sporophytic generation, flowering plants generate male reproductive cells (microsporocytes), which differentiate into multicellular male gametes via meiosis and mitosis during the reduced haploid gametophytic generation (Walbot and Evans, 2003). In higher plants, male reproduction starts with the initiation of the anther primordium, which usually contains three layers, L1, L2, and L3. It is assumed that L1 differentiates into the epidermis, and L2 differentiates into sporogenous cells (microsporocytes) and three inner somatic cell layers: the endothecium, the middle layer, and the tapetum (from outside to the inside) (Ma, 2005; Wilson and Zhang, 2009; Zhang et al., 2011; Feng et al., 2013; Zhang and Yang, 2014). Previous studies hypothesized that a single hypodermal cell beneath the epidermis carries out sequential asymmetric cell divisions to generate three concentric rings of somatic layers and germ cells (Ma, 2005; Feng et al., 2013). However, recent investigations of maize (*Zea mays*) suggest that the peripheral L2-derived (L2-d) cells conduct asymmetric cell division to generate the two distinct cell types: the endothecium and secondary parietal cell (SPC), and then SPCs undergo subsequent symmetric cell divisions to produce the middle layer and the tapetum. The central L2-d cells produce enlarged sporogenous cells (Kelliher and Walbot, 2011).

Recent genetic and biochemical evidence suggests that redox status modulators, transcription factors, receptor-like protein kinases, and small peptides have roles as molecular switches in specifying the cell fate of somatic tissues and germ lines in plants (Zhang and Yang, 2014). Through modulating cellular redox, *Arabidopsis thaliana* CC-type glutaredoxins ROXY1 and ROXY2 (Murmu et al., 2010; S. Li et al., 2011), maize Male Sterile Converted Anther 1 (Chaubal et al., 2003), and rice (*Oryza sativa*) MICROSPORELESS1 (MIL1) (Hong et al., 2012a) can induce the centrally positioned anther precursor cells to gain the identity of archesporial cells, the precursors of male reproductive cells. Mutations in these genes cause the failure to differentiate into archesporial cells during early anther development. In *Arabidopsis*, SPOROCYTELESS (SPL)/NOZZLE is required for sporogenous cell formation, and BARELY ANY MERISTEM1 (BAM1) and BAM2 promote somatic cell fate by limiting the expression of *SPL*. In *spl* mutants, sporogenous cell generation is impaired, and *bam1 bam2* mutants produce extra pollen mother cells at the expense of adjacent somatic cells (Schiefthaler et al., 1999; Yang et al., 1999; Hord et al., 2006; Liu et al., 2009).

Plasma membrane–localized leucine-rich repeat receptor-like kinases, including *Arabidopsis* EXCESS MICROSPOROCYTES1 (EMS1; also known as EXTRA SPOROGENOUS CELLS [EXS]) (Canales et al., 2002; Zhao et al., 2002), SOMATIC EMBRYOGENESIS RECEPTOR LIKE KINASE1 (SERK1) or SERK2 (Albrecht et al., 2005; Colcombet et al., 2005), and the small peptide ligand for EMS1 and SERK1/2, TAPETAL DETERMINANT1

[1] Address correspondence to wqliang@sjtu.edu.cn.
The author responsible for distribution of materials integral to the findings presented in this article in accordance with the policy described in the Instructions for Authors (www.plantcell.org) is: Wanqi Liang (wqliang@sjtu.edu.cn).
[C] Some figures in this article are displayed in color online but in black and white in the print edition.
[W] Online version contains Web-only data.
www.plantcell.org/cgi/doi/10.1105/tpc.114.123745

(TPD1) (Yang et al., 2003, 2005), determine the number of cells in microsporocytes and tapetal cell fate. TPD1-like small peptides are mainly expressed in microsporocytes and likely secreted into the interface between the tapetum and male reproductive cells to interact and form a receptor complex with the leucine-rich repeat receptor-like kinases, thus determining cell fate of the tapetal layer (Zhao et al., 2008). Mutants of these genes produce supernumerary microsporocytes but lack the tapetal layer. Another receptor kinase, RECEPTOR-LIKE KINASE2 (RPK2) has been proposed to be needed for the cell fate specification of the middle layer. Mutation in *RPK2* leads to loss of the middle layer and male sterility (Mizuno et al., 2007).

EMS1/EXS-TPD1–like signaling pathways play a conserved and diversified role in specifying the cell fate and number of anther wall cell layers and microsporocytes. Evidence came from the analysis of the mutants of *TPD1* orthologs such as rice *TPD1-LIKE1A/MIL2* (Hong et al., 2012b) and maize *MULTIPLE ARCHESPORIAL CELLS1* (*MAC1*) (Wang et al., 2012), as well as the rice homolog of the *Arabidopsis EMS1/EXS* genes, *MULTIPLE SPOROCYTE1* (*MSP1*) (Nonomura et al., 2003). *MSP1* expresses not in the sporocytes, but in cells neighboring the male and female sporocytes, and *msp1* has defects in anther and ovule development (Nonomura et al., 2003; Zhao et al., 2008). This is in contrast to the function of its *Arabidopsis* counterpart, *ems1/exs*, which shows no defect in female reproduction (Canales et al., 2002; Zhao et al., 2002). *MIL2* is mainly expressed in inner parietal cells, and the *mil2* mutant only has two anther wall layers, a phenotype which resembles that of *msp1* but differs from that of the *Arabidopsis ems/exs* and *tpd1* mutant (Nonomura et al., 2003; Hong et al., 2012b). Unlike the role of *Arabidopsis TPD1*-like genes in restricting *trans*-differentiation of tapetal cells into meiocytes, maize *MAC1* suppresses archesporial cell proliferation and promotes periclinal division of subepidermal cells; *mac1* displays overproliferation of archesporial cells in both anther and ovule (Wang et al., 2012). These differences in mutant phenotypes imply that species-specific ligand-receptor coordination mechanisms function in regulating the formation of anther wall layers and reproductive cells.

The four somatic helper tissues enclose microsporocytes and support gametogenesis for successful male reproduction in plants (Ma, 2005). They develop into cell layers with distinct cell morphology and function. However, in contrast to the progress on understanding the asymmetric and/or symmetric cell division, when differentiation of somatic cell layers is initiated and how this process is regulated remain largely unknown. Several transcriptional factors that regulate tapetal fate have been identified. An *Arabidopsis* basic helix-loop-helix (bHLH) transcription factor DYSFUNCTIONAL TAPETUM1 (DYT1) and its rice ortholog UNDEVELOPED TAPETUM1 (UDT1) are required for the differentiation of tapetum. In *dyt1* and *udt1* mutants, tapetal cells become abnormally vacuolated and hypertrophic later (Jung et al., 2005; Zhang et al., 2006; Feng et al., 2012). How DYT1 and UDT1 regulate tapetum differentiation is unknown. MYB33/65 (Millar and Gubler, 2005) and the rice protein GAMYB (Kaneko et al., 2004; Tsuji et al., 2006; Aya et al., 2009; Liu et al., 2010), together with TAPETUM DEGENERATION RETARDATION (TDR) (N. Li et al., 2006; Zhang et al., 2008), are positive regulators of tapetum programmed cell death (PCD). Mutation in these genes leads to a vacuolated and hypertrophic tapetum, similar to the phenotype observed in *dyt1* and *udt1* mutants. Whether these genes play a role in tapetum differentiation is unknown.

In this work, we demonstrate that rice TDR INTERACTING PROTEIN2 (TIP2), a bHLH transcription factor, controls cell differentiation and morphogenesis of the endothecium, the middle layer, and the tapetum and regulates normal meiosis and microspore release from the tetrad. Moreover, TIP2 directly activates the expression of *TDR* and *ETERNAL TAPETUM1* (*EAT1*), two key regulators of tapetum development and degradation at later stages. This finding establishes TIP2 as an indispensable switch and reveals a regulatory cascade initiated by TIP2 in controlling anther development in rice.

RESULTS

Identification of the *tip2* Mutant

To identify genes involved in male reproduction in rice, we isolated a male sterile mutant from our rice mutant library generated from an *O. sativa* ssp *japonica* cultivar, 9522 (Chen et al., 2006). The mutant was later named *tip2* after the cloning of the gene and the finding that the gene product interacted with TDR (see below). Compared with the wild type, *tip2* has normal vegetative growth, inflorescence and flower morphology (Figures 1A and 1B). However, *tip2* has smaller anthers and does not produce mature pollen grains during reproductive stage (Figures 1C and 1D), suggesting that the *TIP2* gene is specifically required for male reproduction in rice. When *tip2* plants were backcrossed to wild-type plants, all F1 progenies were fertile, and F2 plants

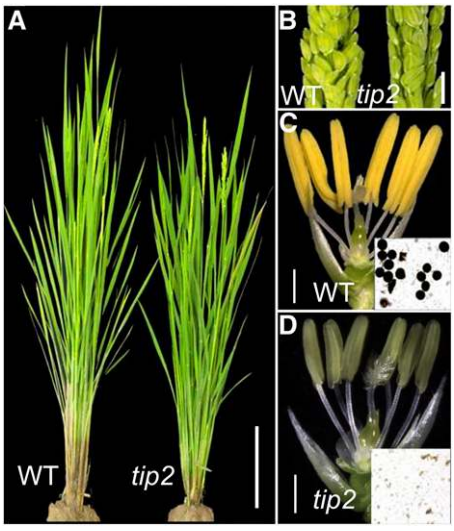

Figure 1. Phenotypic Analysis of *tip2*.

(A) Wild-type and *tip2* plants at stage 12.
(B) Wild-type and *tip2* inflorescences at stage 12 of anther development.
(C) and **(D)** Wild-type and *tip2* flowers showing anthers after removal of the lemma and the palea at stage 12 of anther development. Insets show stained pollen grains.
Bars = 10 cm in **(A)**, 2 cm in **(B)**, and 5 mm in **(C)** and **(D)**.

displayed a segregation of 192 wild-type and 68 mutant plants (3:1, $\chi^2 = 0.184 < \chi^2_{0.05,1} = 3.84$), suggesting that *tip2* is a single recessive mutation.

TIP2 Promotes Cell Differentiation in the Three Inner Anther Wall Layers

To further analyze the defect of *tip2* anthers, we examined transverse sections of mutant anthers. At stage 6 of anther development, the wild-type anther formed four somatic layers (Figure 2A). At stage 7, each cell layer of the wild type showed characteristic cell morphology (Figure 2B): Cells in the epidermis and endothecium cell layers appeared a rectangular shape with transparent cytoplasm and globular nuclei; the middle layer became flattened; tapetal cells with densely staining cytoplasm displayed a square shape. At stage 8, both the endothecium and the middle layer became condensed (Figure 2C). However, the three inner somatic layers of *tip2* anthers displayed no obvious difference in cell shape during stages 6 to 8 (Figures 2D to 2F). Moreover, after meiosis the wild-type middle layer and tapetum disintegrated (Figures 2C and 2G to 2I). However, *tip2* had a vacuolated and expanded cell appearance of the three inner layers and degenerated microspore mother cells, which could not develop into viable pollen grains (Figures 2F, 2J, to 2L).

To characterize *tip2* defects in anther wall layer specification in more detail, we performed 4′,6-diamidino-2-phenylindole (DAPI) staining of cross-sectioned anthers. At stage 6, the three inner anther wall layers of the wild type and *tip2* exhibited similar morphology, as revealed by staining of nuclei (Figures 3A and 3D). Starting from stage 7, the wild type displayed flattened nuclei in the middle layer (Figure 3B). At stage 8 in the wild type, bright DAPI signals can be observed in the two outer layers, but only weak DAPI staining signals can be detected in the tapetum, and

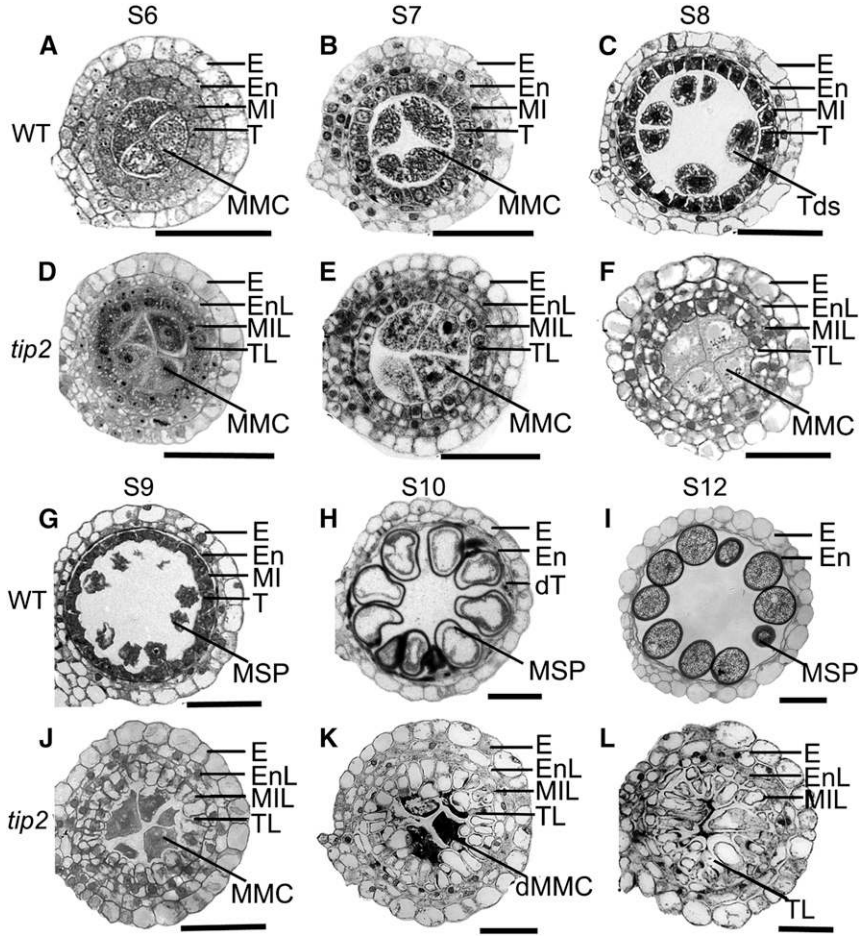

Figure 2. Defects of Anther Wall and Pollen Development in *tip2*.

Semi-thin section analysis of anthers from stage 6 to stage 12 of anther development. The images are cross sections of a single locule. Wild-type anthers are shown in **(A)** to **(C)** and **(G)** to **(I)**, and *tip2* anthers are shown in **(D)** to **(F)** and **(J)** to **(L)**. At stage 6, cell numbers of *tip2* innermost three layers were 16.3 ± 1.6, 18.4 ± 2.0, and 22.0 ± 3.0, respectively; and 15.9 ± 1.6, 17.9 ± 2.0, and 21.4 ± 1.9 for the wild type.

E, epidermis; En, endothecium; MI, middle layer; T, tapetum; Msp, microspore; MMC, meiocyte mother cell; Tds, tetrads; EnL, endothecium-like structure; MIL, middle layer–like structure; TL, tapetum-like structure; dMMC, degenerated MMCs. S6 to S12 refer to stages 6 to 12 of anther development. Bars =15 μm.

the middle layer appeared to have degenerated (Figure 3C). However, from stage 7 to stage 8, the three inner anther wall layers in *tip2* remained undifferentiated, resembling cell morphology to that of wild-type cells at stage 6 (Figures 3A, 3E, and 3F).

Furthermore, DAPI staining showed that *tip2* meiocytes have normal meiosis initiation. At early stage 7, chromosomes featured in meiosis can be observed in both wild-type and *tip2* meiocytes. Meiosis in *tip2* progressed normally from leptotene stage to metaphase I, but arrested at anaphase I and no cytokinesis happened at prophase II. Eventually, *tip2* meiocytes degenerated and did not form tetrads and pollens (Supplemental Figure 1), suggesting that mutation in *TIP2* does not directly affect meiotic initiation but causes the arrest of meiosis.

Transmission electron microscopy (TEM) analysis was conducted to observe in detail the cellular changes in the inner anther wall layers of *tip2* mutants. At stage 6, cells in the three inner somatic layers appeared a similar shape and were occupied by a large nucleus (Supplemental Figures 2A to 2D). At stage 7 when meiosis initiated, wild-type anthers contained four somatic layers with unique features in each layer. Cells in both the middle-layer and tapetum had dense cytoplasm, abundant endoplasmic reticulum, and mitochondria (Figures 4B and 4C).

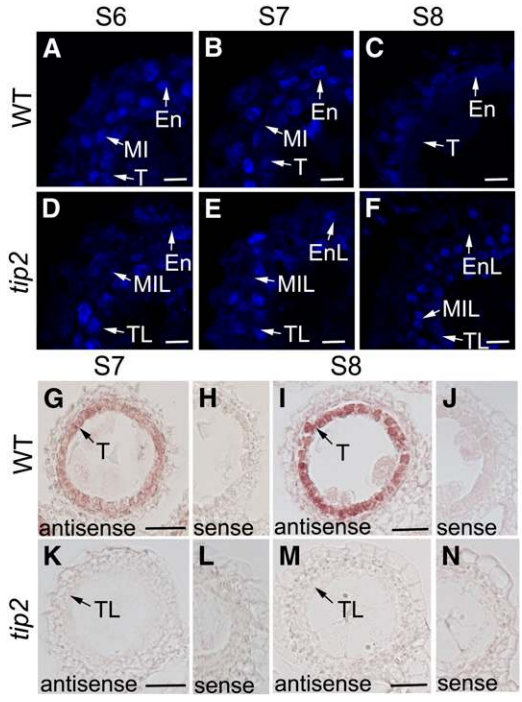

Figure 3. Defects of Anther Wall Differentiation in *tip2*.

(A) to **(F)** Cross section of rice anthers stained with DAPI.
(G) to **(N)** In situ hybridization by the tapetum-specific probe *LTP45*.
E, epidermis; En, endothecium; MI, middle layer; T, tapetum; Msp, microspore; MMC, meiocyte mother cell; Tds, tetrads. EnL, endothecium-like structure; MIL, middle layer–like structure; TL, tapetum-like structure. S6 to S8 refer to stages 6 to 8 of anther development. Bars = 4 μm in **(A)** to **(F)** and 15 μm in **(G)** to **(N)**.

Tapetal cells also had numerous vesicles and small vacuoles scattered throughout the cytoplasm, indicating active metabolism (Figure 4B), the middle-layer cells became significantly compressed with cytoplasm occupied by large vacuoles (Figure 4C), and the endothecium had abundant organelles, such as chloroplasts that contained starch granules (Figure 4D). In *tip2* anthers, although the three inner layers exhibited similar features to that of the wild type at stage 6 (Supplemental Figures 2A to 2H), at stage 7, these cells remained undifferentiated and contained a large number of proplastid-like organelles (Figures 4E to 4H). These results supported the role of TIP2 in promoting cell differentiation of the three inner anther wall layers. Unlike the condensation and degeneration of wild-type tapetal cells at late stage 8 and stage 9, *tip2* tapetal cells became significantly expanded (Figures 4I to 4L; Supplemental Figures 2I to 2X).

To further confirm the cell identity of inner anther wall layers in *tip2*, we detected the expression of a rice tapetum marker gene, *LIPID TRANSFER PROTEIN45* (*LTP45*), in these cells. *LTP45* is a homolog of *Arabidopsis A9*, a tapetum-specific marker for early anther developmental stages (Paul et al., 1992). *LTP45* was preferentially expressed in tapetal cells at stage 7 and stage 8 in wild-type anthers, whereas in *tip2* anthers its expression was not detectable (Figures 3G to 3N), suggesting that *tip2* has defects in tapetal cell identity specification. We were unable to analyze the identity of the endothecium and middle layer due to lack of marker genes for these two layers in plants.

In addition, we observed extra periclinal division in *tip2* tapetum-like layer at stage 8, with an average frequency of 3.68 ± 2.8 cells per locule (n = 71) (Supplemental Figure 3A; Figures 4J and 4L), which was not seen in wild-type anthers (n = 30). Consistent with this, the average cell number of *tip2* tapetum-like layer had a significant increase (30.1 ± 4.4, n = 71) compared with the wild type (25.1 ± 1.9, n = 30) at stage 8 ($Z = 14.3 > Z_{0.05} = 1.96$), although at stage 6 the average cell numbers of *tip2* innermost three anther wall layers had no significant difference from that of the wild-type plants. DAPI staining observation indicated that the periclinal dividing cells exhibit a mitosis-like pattern (Supplemental Figures 3B to 3D). These results suggested that *tip2* anthers have prolonged periclinal cell division activity after the formation of the inner two anther wall layers via periclinal cell division from SPCs.

TIP2 Promotes Tapetal PCD and Degeneration of Callose Surrounding the Microspores

Section analysis and terminal deoxynucleotidyl transferase-mediated dUTP nick-end labeling (TUNEL) DNA fragmentation assay was used to monitor PCD in tapetal cells. In the wild type, meiocytes formed tetrads after meiosis, tapetal cells became condensed and initiated PCD-promoted degeneration, and the middle layer also started to be degraded (Figures 2C and 5A) (N. Li et al., 2006; Niu et al., 2013). By contrast, cell morphology of the three inner anther wall layers of *tip2* anthers remained similar, and no obvious tapetal PCD signals were detected (Figures 2F and 5A), suggesting that TIP2 is a positive regulator of tapetal PCD.

Tapetal cells secrete β-1,3-glucanase (callase), which can degenerate the callose wall outside tetrads to release young microspores (Ariizumi and Toriyama, 2011). Cross section of anthers stained by aniline blue showed deposition of callose around the

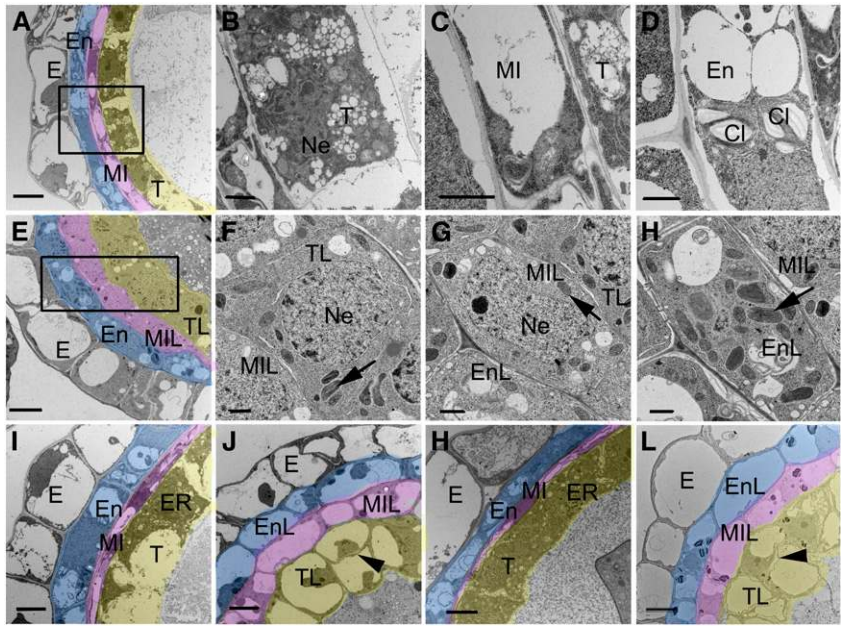

Figure 4. TEM Analysis of *tip2* Anthers.

(A) to **(H)** Transverse section of wild-type (**[A]** to **[D]**) and *tip2* (**[E]** to **[H]**) anthers at stage 7. **(B)** to **(D)** and **(F)** to **(H)** are higher magnification of blank region in **(A)** and **(E)**, showing tapetum (**[B]** and **[F]**), middle layer (**[C]** and **[G]**), and endothecium (**[D]** and **[H]**), respectively.
(I) and **(J)** Transverse section of wild-type **(I)** and *tip2* **(J)** anthers at stage 8.
(K) and **(L)** Transverse section of wild-type **(K)** and *tip2* **(L)** anthers at stage 9.
E, epidermis; En, endothecium; MI, middle layer; T, tapetum; Msp, microspore; MMC, meiocyte mother cell; Tds, tetrads. EnL, endothecium-like structure; MIL, middle layer–like structure; TL, tapetum-like structure; Ne, nucleus; Cl, chloroplast; ER, endoplasmic reticulum. Arrowhead shows an extra layer of tapetum-like structures in *tip2* mutant. Arrow shows proplastid-like structure in the innermost three layers in *tip2* mutant. Bars = 5 μm in **(A)**, **(E)**, and **(I)** to **(L)** and 1 μm in **(B)** to **(D)** and **(F)** to **(H)**.

meiocytes in both the wild type and *tip2* at stages 7 and 8 of anther development (Figure 5B). However, in stark contrast to the degradation of callose enclosing wild-type microspores, *tip2* displayed undegenerated callose around meiocytes, suggesting defective callose degeneration in the *tip2* mutant.

TIP2 Encodes a bHLH Transcription Factor

To identify the *TIP2* gene, we employed a map-based cloning strategy. Using an F2 population of 340 individual mutant lines and six InDel markers, we located the *TIP2* locus on chromosome 1 between Z6.1-5 and Z6.2-1, two markers that defined a 170-kb region (Figure 6A). By genomic sequencing of candidate genes within this region, we found a deletion of two continuous G nucleotides in the second exon of *Os01g0293100*, resulting in a frame shift of the protein (Figure 6B). Transgenic *tip2* plants expressing *TIP2* wild-type genomic DNA recovered male fertility (Supplemental Figure 4), demonstrating that *Os01g0293100* is responsible for the male sterile phenotype in *tip2*.

The *TIP2* cDNA encodes a putative bHLH transcription factor containing a conserved bHLH domain and a Domain Unknown Function domain, which shares high sequence similarity with *EAT1* and is homologous to *Arabidopsis AtbHLH010*, *AtbHLH089*, and *AtbHLH091* (X. Li et al., 2006; Niu et al., 2013). We observed the localization of TIP2 protein using transgenic rice plants expressing a *TIP2cds-eGFP* fusion driven by 35S promoter. Stably expressed TIP2 fused with GFP was observed in nuclei of root cells (Supplemental Figure 5).

TIP2 Expresses Specifically in the Endothecium, Middle Layer, and Tapetum

To further investigate the function of *TIP2*, we analyzed the expression pattern of *TIP2* in different tissues using quantitative RT-PCR (qRT-PCR). *TIP2* expression was specifically observed in anthers, from the meiosis stage to mitosis, with a maximum expression level at stages 7 and 8. This expression pattern is consistent with the defects shown in *tip2*. Interestingly, *tip2* anthers displayed a lower level of *TIP2* than the wild type from stage 6 to stage 8, but a higher level than the wild type after stage 9, when young microspores were released (Figure 7A), suggesting a possible feedback regulation of *TIP2* transcription. Furthermore, in situ hybridization showed strong expression of *TIP2* in the middle layer and tapetum and weak expression in the endothecium in the wild type (Figures 7B and 7C). By contrast, only background signal was detected in the same anther section with the sense probe (Figure 7D). We also detected expression of *TIP2* in meiocytes at stages 7 and 8, when meiosis initiated (Supplemental Figure 6). These results supported the role of TIP2 in specifying the cell pattern of inner anther walls and functioning in meiosis progression.

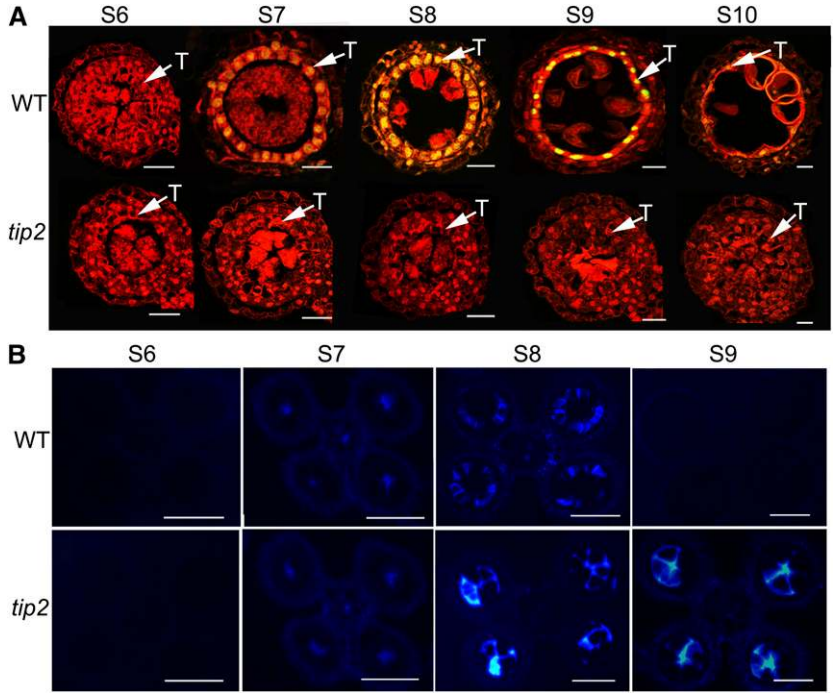

Figure 5. Defective Tapetal PCD and Callose Degeneration in *tip2*.

(A) TUNEL assay of anthers. The red signal is propidium iodide staining. Yellow color represents the overlap of TUNEL and PI signals.
(B) Aniline blue staining of anther sections.
T, tapetum; S6 to S10 represent stages 6 to 10 of anther development. Bars = 10 μm in **(A)** and 50 μm in **(B)**.

TIP2 Interacts with TDR to Promote Tapetum Differentiation

It has been shown that bHLH transcriptional factors function as homodimers or heterodimers (Firulli et al., 2000). We previously reported that the bHLH protein ABORTED MICROSPORES (AMS), a key regulator of tapetum development and degradation, can interact with AtbHLH089 and AtbHLH091, two homologs of TIP2 in *Arabidopsis* (Sorensen et al., 2003; Xu et al., 2010; Ma et al., 2012). Consistent with this, TDR, the rice ortholog of AMS, interacts with EAT1, the paralog of TIP2 in vitro and in vivo (Niu et al., 2013). To understand whether TIP2 physically interacts with TDR or EAT1, yeast two-hybrid analysis was used. Yeast strains coexpressing TIP2 and TDR grew normally on medium lacking His and Ade in the presence of 10 mM 3-aminotriazole and displayed activation of the expression of the LacZ reporter genes, which confirmed the interaction between TIP2 and TDR (Figure 8A). In contrast, yeast strains coexpressing TIP2 and EAT1 failed to grow under the same selection conditions lacking His and Ade in the presence of 10 mM 3-aminotriazole (Supplemental Figure 7A), suggesting no interaction between TIP2 and EAT1. The interaction between TIP2 and TDR as well as no interaction between TIP2 and EAT1 were further confirmed using in vitro pull-down assay (Figure 8B; Supplemental Figure 7B).

Our previous study showed that *TDR* is preferentially expressed in tapetum at stages 7 to 9 and mutation in *TDR* affects the tapetum PCD (N. Li et al., 2006). The interaction of TDR with TIP2 suggests that TDR may play a role at earlier developmental stages. We reexamined the phenotypes of *tdr* at stages 7 and 8 using TEM and DAPI staining. *tdr* displayed normally characteristic endothecium and middle layer but less differentiated tapetal cells at stage 7 (Supplemental Figures 8A to 8F and Supplemental Figure 9A), and innermost three layers became vacuolated and expanded at stage 8 (Supplemental Figures 8G to 8L). Also, we observed a substantial decrease in transcript levels of the rice tapetum-specific gene *LTPL45* in *tdr*, as we

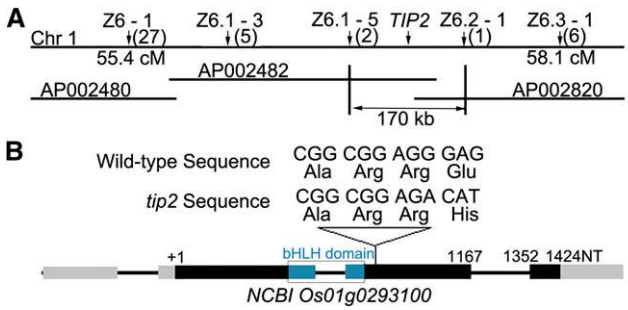

Figure 6. Molecular Identification of *TIP2*.

(A) Fine mapping of *TIP2*. Markers used for the mapping are indicated. Numbers in parentheses indicate the number of recombinants. AP002480, AP002482, and AP002820 are access numbers of BACs.
(B) Schematic representation of *TIP2*. Black rectangles represent exons, gray rectangles represent untranslated region.
[See online article for color version of this figure.]

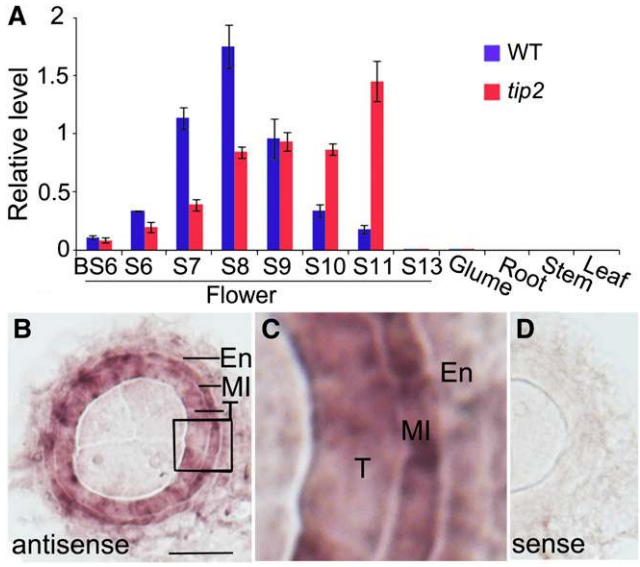

Figure 7. Expression Analysis of *TIP2*.

(A) Expression analysis of *TIP2* using qRT-PCR. RNA was extracted from whole flowers before stage 7 and from anthers after stage 7. Error bars refer to SD of three biological repeats.
(B) In situ hybridization analysis of *TIP2* in wild-type anther at stage 6.
(C) Magnification of the squared region in **(B)**.
(D) The same sample in **(B)** probed by the sense probe as negative control.
EN, endothecium; MI, middle layer; T, tapetum. BS6, before stage 6; S6 to S13 refer to stages 6 to 13. Bar = 15 μm in **(B)**.

also observed in *tip2* anthers. In contrast, no significant expression change of *LTP45* was detected in *eat1* at stage 7, but *LTP45* transcript levels increased at stage 8 (Supplemental Figure 9B). Those similar properties of defective tapetum in both *tip2* and *tdr* indicated that TIP2 may cooperate with TDR in regulating early tapetal cell differentiation.

TIP2 Regulates *TDR* and *EAT1*

To further investigate the regulatory function of *TIP2*, we performed qRT-PCR to analyze the expression level of genes involved in tapetum development and degradation. The expression level of transcription factors *TDR*, *EAT1*, and *PERSISTENT TAPETAL CELL1* (*PTC1*) (H. Li et al., 2011) decreased significantly in *tip2* compared with that in wild-type plants (Figure 9A; Supplemental Figure 10). By contrast, *UDT1* (Jung et al., 2005), another key regulatory bHLH transcription factor, was upregulated in *tip2*. *GAMYB* showed little difference in expression level at meiosis stage and slightly increase after meiosis (Supplemental Figure 10). These results suggested that TIP2 may positively regulate the expression of *TDR*, *EAT1*, and *PTC1* in tapetum. UDT1 and GAMYB could be involved in parallel regulatory pathways.

bHLH transcription factors regulate gene transcription by binding to the E-box (CANNTG) in the promoter region of target genes (Xu et al., 2010). Therefore, we next used quantitative chromatin immunoprecipitation (qChIP)-PCR to determine whether TIP2 directly regulates these genes. We produced TIP2 polyclonal antibodies against a peptide that corresponds to amino acids 1 to 102 (see Methods) and determined the specificity of the antibody using protein gel blot assay (Supplemental Figure 11). Our qChIP-PCR results showed that TIP2 could directly bind to the E-box–containing promoter regions of *TDR* and *EAT1* (Figure 9C). The binding of TIP2 to the promoter regions of *TDR* and *EAT1* was confirmed by electrophoretic mobility shift assay (EMSA) using qChIP-PCR enriched promoter regions (Figure 9B).

The *tdr* mutant plants display normally characteristic endothecium and middle layer but expanded tapetum and retarded tapetal PCD (N. Li et al., 2006). The *eat1* mutants exhibit well developed innermost three anther wall layers but delay in tapetal PCD (Niu et al., 2013). Moreover, *tdr eat1* double mutants show defects similar to *tdr* single mutant, and *EAT1* is downregulated in *tdr* (Niu et al., 2013). To determine the genetic interaction among TDR, EAT1, and TIP2, we constructed double mutants *tdr tip2* and *tip2 eat1*. Histological analysis showed that both double mutants displayed aborted meiocytes, abnormal development of the three inner layers, and expanded tapetum-like cells in anthers, which was similar to the phenotype of the *tip2* single mutant (Figure 9D; Supplemental Figure 12). Therefore, our results supported the idea that *TIP2* acts upstream of *TDR* and *EAT1*.

Consistent with the downregulation of *TDR* and *EAT1*, we also detected the decreased expression of a cysteine protease-encoding gene, *CP1*, and two aspartic protease-encoding genes, *AP25*

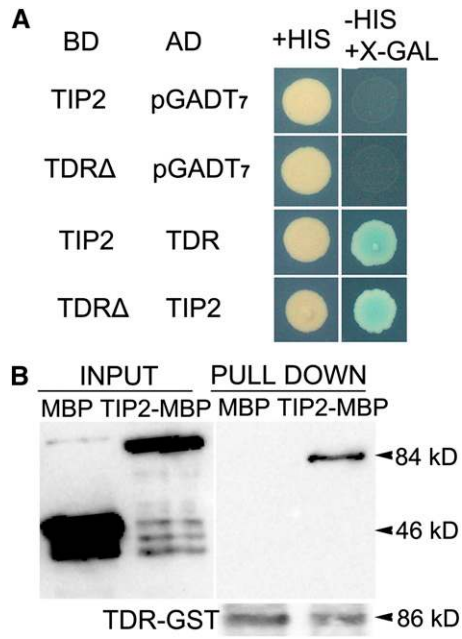

Figure 8. Interaction between TDR and TIP2.

(A) Yeast two-hybrid assays to detect interactions between TIP2 and TDR. Empty vector $pGADT_7$ was used as the control.
(B) Immunoblotting analysis of in vitro–translated full-length TIP2 pulled down by the GST-tagged TDR protein. MBP tag alone was used as a negative control to show no interaction between MBP and the GST tag.

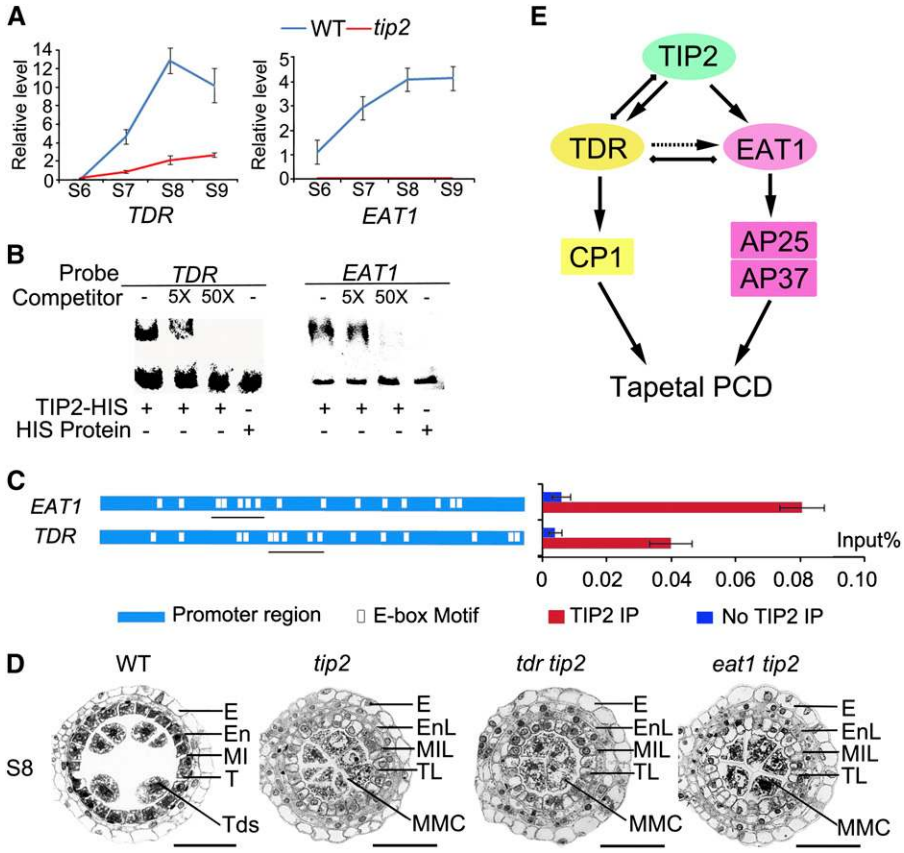

Figure 9. TIP2 Acts Upstream of TDR and EAT1.

(A) qRT-PCR analysis of *TDR* and *EAT1* in *tip2* anthers. Error bars refer to SD of three biological repeats.
(B) EMSA assay of the binding of recombinant TIP2 to the E-box–containing promoter fragments of *EAT1* and *TDR*. Unlabeled competitors were added at 5- or 50-fold concentration compared with labeled probes.
(C) qChIP-PCR analysis of the enrichment of TIP2 with the promoter regions of *TDR* and *EAT1* in flowers at stage 7 of anther development. Distribution of E-box motifs in the promoter regions of *TDR* and *EAT1* is indicated (left), and their enrichment compared with the input sample was tested by qChIP-PCR. Error bars refer to SD of three biological repeats.
(D) Semi-thin section analysis of anthers at stage 8. E, epidermis; En, endothecium; MI, middle layer; T, tapetum; Msp, microspore; MMC, meiocyte mother cell; Tds, tetrads. EnL, endothecium-like structure; MIL, middle layer–like structure; TL, tapetum-like structure. S6 to S9 refer to stages 6 to 9 in anther development. Bars = 15 μm.
(E) Schematic representation of TIP2 in promoting tapetal PCD by directly regulating the expression of *TDR* and *EAT1*.

and *AP37* (Supplemental Figure 13). *CP1* is required for anther development, and its expression is directly regulated by TDR (Lee et al., 2004; N. Li et al., 2006), and *AP25* and *AP37* are directly regulated by EAT1 (Niu et al., 2013).

In agreement with the *tip2* defect in callose degradation, we detected reduced expression of three glucanase-encoding genes putatively related to callose degradation, including *G1* (Wan et al., 2011), and two homologs of *Arabidopsis A6* (Hird et al., 1993) in rice, *Os09g32550* and *Os08g41410* (Supplemental Figure 13). In addition, other genes involved in tapetum late function, including those related to lipid metabolism and transport, such as *CYP703A3* (Aya et al., 2009), *CYP704B2* (Li et al., 2010), *C6* (Zhang et al., 2010), and *DEFECTIVE POLLEN WALL* (*DPW*) (Shi et al., 2011), also exhibited significantly decreased transcription in *tip2* (Supplemental Figure 13). These results suggested the presence of a TIP2-mediated transcription cascade that regulates tapetum development and degeneration in rice.

DISCUSSION

TIP2 Plays a Key Role in Specifying Cell Pattern of Three Inner Anther Somatic Layers

Timely cell differentiation is of critical importance for the patterning of plant organs. In this study, we demonstrate that TIP2 plays a key role in controlling cell differentiation of inner anther wall layers during early anther development. Even though *tip2* anthers seem to be able to undergo normal cell division in generating four anther wall layers from the precursor cells, incomplete differentiation of the three inner anther wall layers and

even extra tapetal cell division occur in the mutant (Figures 2 to 4). Therefore, our findings demonstrate that TIP2 is a key regulator in suppressing the proliferation of meristemoid cells and promoting acquisition of cell identity in the three inner anther wall layers during early anther development.

The precursor cells (primary parietal cells [PPCs]) of the inner three somatic cell layers are formed by asymmetric cell division of L2-d cells or alternatively adopting somatic fate by the instruction of centrally localized L2-d cells (Zhang and Yang, 2014). PPCs undergo two more rounds of periclinal cell division: The first round of division generates two secondary parietal cell layers, and the inner SPC layer subsequently divides into two somatic cell layers. Our detailed observations revealed that in rice, the newly formed cell layers display similar morphological and cellular features at stage 6 (Supplemental Figures 2A to 2D) and establish distinct characteristics at stage 7 when meiocytes enter meiosis (Figures 4A to 4D). These observations indicate that differentiation of L2 derived somatic cells starts nearly simultaneously and an early endothecium cell-like feature might be the default status of these cells. In *tip2*, three inner anther wall layers exhibited no difference compared with those of the wild type till stage 6 (Supplemental Figures 2E to 2H), suggesting that TIP2 is not required for the periclinal divisions and early cell fate decision. But development of these cell layers is arrested and deviated from that of wild type after stage 6 (Figures 4E to 4H), implicating the essential role of TIP2 in cell patterning. Consistently, *TIP2* transcripts can be detected in the newly formed endothecium, middle layer, and tapetum at stage 6, but not in the PPCs and SPCs (Figures 7B to 7D).

Several of the signaling components involved in rice early anther cell fate determination display a similar spatial expression pattern before the meiosis stage. *MSP1* and *MIL2* are first expressed in archesporial cells then preferentially in PPCs and SPCs, later gradually confined to the middle layer and the tapetum. This spatial distribution pattern suggests that MSP1 and MIL2 may regulate both the generation and differentiation of the three inner anther wall layers (Nonomura et al., 2003; Hong et al., 2012b). *MIL1* is also expressed in the precursor cells and restricted to the middle layer and tapetum at later developmental stages. In *mil1* mutants, the inner secondary parietal layer can normally divide into two layers, but these two layers fail to differentiate into middle layer and tapetum, indicating that MIL1 is involved in specifying the cell pattern of these two layers in addition to regulating meiosis initiation (Hong et al., 2012a). *TIP2* expresses later than these genes and may act downstream of these regulators. Consistent with this hypothesis, the expression level of *MSP1* and *MIL2* did not show significant changes in *tip2* (Supplemental Figure 10). UDT1 is another early regulator of rice anther development and has an overlapping transcript distribution with *TIP2*. Mutation in *UDT1* results in defective differentiation of inner somatic cell layers (Jung et al., 2005; Hong et al., 2012b). *UDT1* is upregulated in the *tip2* mutant (Supplemental Figure 10), suggesting that they may act in parallel regulatory pathway and the upregulation of *UDT1* may be induced by a feedback signal.

The division of PPCs generates two layers of SPCs, and the inner SPCs obtain meristemoid identity and retain periclinal cell division activity. In wild-type anthers, the two layers derived from the division of inner SPC layer can only divide in an anticlinal manner. By contrast, in *tip2* mutants, extra periclinal cell division can be observed in some cells of the innermost cell layer (Figures 4I to 4L; Supplemental Figure 3A). Similarly, more than four cell layers can be observed in some regions of the *mil1* parietal tissues (Hong et al., 2012a). It seems that after each round of parietal cell division, the inner descendants retain the meristemoid characteristics and the ability to carry on periclinal division. Cell differentiation may be required to halt this cell division activity. However, not all inner cells in *tip2* and *mil1* mutants undergo periclinal division, indicating that cell division and differentiation of the innermost cell layer may be controlled by overlapping regulatory pathways.

TIP2 Regulates Tapetal PCD

Because the innermost anther wall layer is next to the male reproductive cells, the tapetum provides nutritive support for microspore development and pollen wall formation by undergoing a PCD-triggered degradation after meiosis (N. Li et al., 2006; Niu et al., 2013). Premature or retarded tapetal degeneration frequently causes male sterility (N. Li et al., 2006; Li et al., 2007; Zhang et al., 2007; Shi et al., 2009; Phan et al., 2011). Genetic investigations discovered several transcription factors involved in rice tapetal degeneration, such as GAMYB (Kaneko et al., 2004; Liu et al., 2010), TDR (N. Li et al., 2006), EAT1 (Niu et al., 2013), and Os-API5 (X. Li et al., 2011; Zhang et al., 2011). The *tip2* mutant displays uncontrolled tapetum-like cell enlargement and delayed PCD (Figures 2A to 2L and 5A), which is similar to the phenotypes of *gamyb* (Kaneko et al., 2004) and *tdr* mutants (N. Li et al., 2006), but differs from *eat1* (Niu et al., 2013), *ptc1* (H. Li et al., 2011), and *osapi5* (X. Li et al., 2011), in which no obvious cell enlargement was observed. These findings suggest that TIP2,

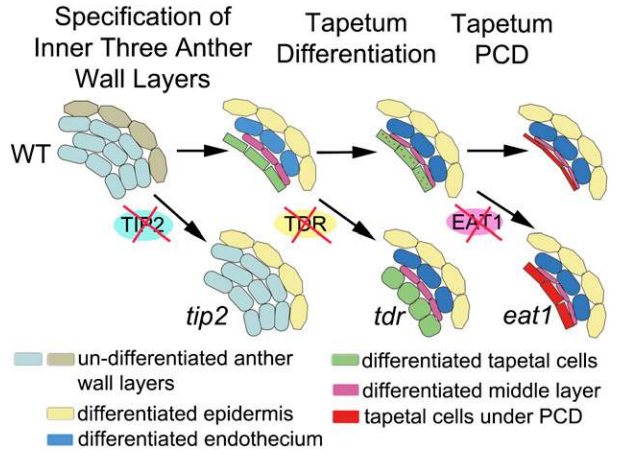

Figure 10. Proposed Model for the TIP2-TDR-EAT1 Cascade That Regulates Anther Wall Cell Fate and Microspore Development in Rice.

TIP2 promotes the specification of anther wall cell identity and differentiation, and loss-of-function of TIP2 results in undifferentiated innermost three layers. TIP2 activates the expression of *TDR* and *EAT1*. TDR plays dual roles in tapetum differentiation and degradation. Mutation in *TDR* leads to abnormally expanded tapetum and delayed PCD. EAT1 plays a major role in triggering tapetal PCD. *eat1* mutants display a persistent tapetal activity and delayed PCD.

GAMYB, and TDR may be required for controlling tapetal cell size and promoting tapetal PCD during rice anther development. Moreover, the major function for EAT1, PTC1, and Os-API5 may be the regulation of tapetal PCD.

Delayed PCD in *tip2* may be an indirect result of the deficiency in cell differentiation. Our analysis revealed that TIP2 can directly activate the expression of *TDR* and *EAT1*, indicating a direct role of TIP2 in promoting PCD. Supportively, our expression analysis revealed that in *tip2*, *CP1*, *AP25*, and *AP37* are downregulated (Supplemental Figure 13).

Consecutive Functions of Three bHLH Transcription Factors in Anther Development

bHLH proteins often function in transcriptional cascades in cell identity specification and differentiation in plants and animals (Weintraub et al., 1991; Pillitteri et al., 2007; Pillitteri and Torii, 2012). Homologous bHLH proteins in animals, such as the four mammalian myogenic regulators, MyoD, Myf-5, myogenin, and MRF4, as well as the achaete–scute complex in *Drosophila melanogaster*, control sequential processes in a hierarchical fashion (Olson, 1990; Campuzano and Modolell, 1992; Weintraub, 1993). In *Arabidopsis*, three closely related bHLH proteins, SPCH, MUTE, and FAMA, are key switches for three key consecutive steps of stomatal formation (Ohashi-Ito and Bergmann, 2006; MacAlister et al., 2007; Pillitteri et al., 2007; Lampard, 2009; Hachez et al., 2011; Triviño et al., 2013)

Our previous work shows that, phylogenetically, TIP2, EAT1, and TDR are closely grouped (X. Li et al., 2006), and they might be generated by gene duplication during evolution. This work and our previous discovery reveal that these three bHLH proteins display successive expression patterns and have overlapping and divergent functions during anther development (Figure 10) (N. Li et al., 2006; Niu et al., 2013). *TIP2* expresses in the endothecium, the middle layer, and the tapetum from stage 6 to stage 10, and these three inner anther wall layers are undifferentiated in *tip2* mutants, suggesting the role of TIP2 in specifying cell pattern of the endothecium, the middle layer, and the tapetum in early anther development. In addition, TIP2 is required for the activation of late function genes in tapetum. *TDR* highly expresses from stage 7 to stage 9 and specifically in the tapetum and plays dual role in promoting tapetum differentiation and degradation. *EAT1* highly expresses at stage 8 to stage 10, mainly in tapetum, and *eat1* mutants show three well developed inner cell layers but delayed tapetal PCD, suggesting that EAT1 may play a major role in triggering tapetal PCD in anthers (Figure 10).

Our previous expression and genetic analyses show that *TDR* acts upstream of *EAT1*. *EAT1* expression is reduced in *tdr*, but *TDR* expression is not changed in *eat1*. Moreover, the *tdr eat1* double mutant exhibits the defects similar to *tdr*, suggesting that the function of *EAT1* relies on a functional TDR protein (Niu et al., 2013). In this study, we show that TIP2 directly activate the expression of *TDR* and *EAT1* and physically interact with TDR. Therefore, we propose that the three closely related bHLH proteins, TIP2, TDR, and EAT1, might have evolved by gene duplication and their expression and function in anther pattern formation underwent diversification during evolution. TIP2 can promote cell differentiation of three inner somatic cells. TIP2 initiates the expression of *TDR* and *EAT1* and interacts with TDR. TDR regulates tapetal differentiation and promotes tapetal PCD. Finally, TDR interacts with EAT1, and EAT1 triggers cell death in the tapetum. Together, TIP2, TDR, and EAT1 are components of a sequential regulatory cascade for anther wall layer development (Figure 10).

In summary, we demonstrate TIP2 as a new regulator of cell patterning of three inner somatic anther wall layers and the microspore development in rice. Three bHLH proteins, TIP2, TDR, and EAT1, form a sequential regulatory cascade in regulating consecutive steps including cell differentiation, cell morphogenesis, and cell death during anther development. This finding provides new insights into the role of bHLH proteins in plant reproduction.

METHODS

Plant Materials, Growth Conditions, and Molecular Cloning of *TIP2*

Rice (*Oryza sativa*) plants used in this study are in the 9522 background (*O. sativa* ssp *japonica)* and were grown in the paddy field of Shanghai JiaoTong University. F2 progenies for mapping were generated by a cross between wild-type *GuangLuAi* species (*indica*) and the *tip2* mutant (*japonica*). Male sterile plants in the F2 population were selected for mapping. To map the *TIP2* locus, bulked segregated analysis was used and 24 pairs of InDel molecular markers were designed based on the sequence difference between *japonica* and *indica*. Further fine-mapping of *TIP2* was performed using the previously published method (Chu et al., 2005).

Characterization of Mutant Plant Phenotypes

DAPI staining of microspores was performed as reported (Wang et al., 2010). TEM, callose staining, TUNEL assay, and semi-thin section analysis were performed according to a previous study (Tan et al., 2012). Anthers from different developmental stages, as defined by Zhang et al. (2011), were collected based on the comparison and analysis of wild-type and *tip2* plants on glume length and morphology (Supplemental Figure 14), and the developmental stages of wild-type anthers were further confirmed by semi-thin section.

Complementation of *tip2*

A 4.8-kb genomic sequence of *TIP2* including the entire *TIP2* coding region, 3.1-kb upstream sequence, and 0.5-kb downstream sequence was amplified using a BAC that contained *TIP2* as the template. The amplified fragment was cloned into the binary vector pCAMBIA1301, which contains a hygromycin resistance gene. Calli induced from young panicles of homozygous *tip2* mutant plants were used for transformation with *Agrobacterium tumefaciens* (EHA105) carrying pCAMBIA1301-*TIP2* plasmid or the control plasmid pCAMIBA1301. Over 50 positive transgenic plants were obtained and confirmed by PCR (primers used are listed in Supplemental Table 1).

qRT-PCR and in Situ Hybridization

Total RNA was isolated using TRI reagent from rice tissues. One microgram of RNA per sample was used to synthesis cDNA using the Primescript RT reagent kit with genomic DNA eraser (Takara). qRT-PCR was performed on a cycler apparatus (Bio-Rad) using SYBR Premix Ex Taq GC (Takara) according to the manufacturer's instructions. Amplification was conducted following this protocol: 95°C for 2 min, 40 cycles of 95°C for 5 s, and 60°C for 35 s. *ACTIN* (Supplemental Table 1) was used as an internal control, and a relative quantitation method (Δ cycle threshold) was used to quantify the

relative expression level of target genes. Three biological repeats with three technique repeats each were included in producing statistical analysis and error range analysis.

In situ hybridization was performed as described by Tan et al. (2012). Two *TIP2* cDNA fragments generated by PCR were used for preparing antisense and sense probes (Supplemental Table 1).

Yeast Two-Hybrid Assays

Yeast two-hybrid assays were performed according to instructions of the Matchmaker GAL4 two-hybrid system (Clontech). Truncated TDR fragment containing the N-terminal bHLH domain (TDR^{Δ}, amino acids 1 to 344) was from Niu et al. (2013). His and Ade selection and X-Gal filter assay were performed according to the manufacturer's instructions.

Pull-Down Assay

TIP2 fused with Maltose Binding Protein (MBP) and TDR fused with glutathione *S*-transferase (GST) were expressed in $BL_{21}DE_3$ *Escherichia coli* cells. Proteins were purified using amylose and GSSH resin, respectively. The eluent was analyzed using 10% SDS-PAGE, according to the method published by Bai et al. (2012). Monoclonal antibodies against MBP (NEB) and GST (Beyotime) were used.

qChIP-PCR and EMSA Analysis

A *TIP2*-specific DNA fragment, which encodes a 102–amino acid peptide (1 to 102), was synthesized in vitro using optimized codons for *E. coli*. Two repeats of this fragments were linked together, fused with the His tag in the pET32a vector, and expressed in *E. coli* ($BL_{21}DE_3$). Full-length TIP2 fused with GST tag in pGEX4T-1 vector was expressed and purified for antibody purification. The specificity of the TIP2 antibody was examined according to the method described by Zhang et al. (2010). The fold enrichment of TIP2 target promoter regions was compared with the input sample, and IgG antibody was added as negative control. Ten biological repeats with three technique repeats each were included in producing statistical analysis.

Full-length TIP2 coding region fused with His-tag was expressed in *E. coli* ($BL_{21}DE_3$). DNA fragments of *TDR* and *EAT* promoter regions, which were positively enriched in qChIP-PCR, were amplified using dig-dNTP (Yinuojin). Experimental procedures of qChIP-PCR and EMSA were performed following the descriptions by Xu et al. (2010).

Accession Numbers

Sequence data from this article can be found in the GenBank/EMBL data libraries under the following accession numbers: *EAT1* (Os04g0599300), *TDR* (Os02g0120500), *GAMYB* (Os01g0812000), *CP1* (Os04g0670500), *AP25* (Os03g0186900), *AP37* (Os04g0448500), *CYP704B2* (Os03g0168600), *CYP703A3* (Os08g0131100), Os-*C6* (Os11g0582500), *UDT1* (Os07g0549600), *LTPL45* (Os09g0525500), *RA68* (Os02g0230300), *DPW* (Os03g0167600), *MSP1* (Os01g0917500), *UGPase 1* (Os09g0553200), *UGPase 2* (Os02g0117700), *G1* (Os01g0947700), *GT1* (Os01g0262600), *PDA1* (Os06g0607700), *PTC1* (Os09g0449000), *MIL2* (Os12g0152500), and *MADS3* (Os01g0201700).

Supplemental Data

The following materials are available in the online version of this article.

Supplemental Figure 1. Analysis of Meiosis in *tip2* by DAPI Staining.

Supplemental Figure 2. TEM Analysis of Anther Wall Cell Differentiation.

Supplemental Figure 3. Tapetum-Like Layer Exhibits Extra Periclinal Cell Division in *tip2*.

Supplemental Figure 4. Complementation of *tip2* by *TIP2* Genomic DNA.

Supplemental Figure 5. Subcellular Localization of TIP2.

Supplemental Figure 6. In Situ Hybridization of TIP2.

Supplemental Figure 7. Analysis of the Interaction between TIP2 and EAT1.

Supplemental Figure 8. TEM Analysis of Undifferentiated Tapetum in *tdr*.

Supplemental Figure 9. Defects of Tapetum Differentiation in *tdr*.

Supplemental Figure 10. Expression Analysis of Reported Genes Involved in Tapetal Development in *tip2* Using qRT-PCR.

Supplemental Figure 11. Specificity Analysis of TIP2 Antibody.

Supplemental Figure 12. Transverse Section Analysis of *eat1 tip2* and *tdr tip2* Anthers.

Supplemental Figure 13. Expression Analysis of Reported Genes Involved in Tapetal PCD, Callose Dissociation and Pollen Development in *tip2* Using qRT-PCR.

Supplemental Figure 14. Size of Flowers and Anthers of Wild Type and *tip2* at Various Development Stages.

Supplemental Table 1. Primers Used in This Study.

ACKNOWLEDGMENTS

We thank Jianping Hu for helpful suggestions on the article and the Rice Genome Resource Center for providing the TIP2 BAC clone. We thank Lu Zhu, Xiaoyan Gao, and Gema Vizcay-Barrena for TEM observation, Changsong Yin for in situ hybridization, Zhijing Luo for mutant screening and generation of F2 population for mapping, and Xiuwen Rao for the construction of TIP2-MBP. This work was supported by funds from National Key Basic Research Developments Program, Ministry of Science and Technology, China Grant 2013CB126902; the 863 High tech Project, Ministry of Science and Technology, China Grant 2012AA10A302; National Natural Science Foundation of China Grants 31322040, 31171518, 31271698, and 31110103915; and Science and Technology Commission of Shanghai Municipality Grant 13JC1408200.

AUTHOR CONTRIBUTIONS

Z.F. carried out major parts of all experiments. J.Y. performed the EMSA analysis. X.C. prepared sections for DAPI staining and in situ hybridization. X.Z. and Z.L. performed DAPI analysis of anther meiocytes. J.X. helped in qChIP-PCR analysis. M.C. screened the *tip2* mutant and generated F2 population for mapping. D.Z. and W.L. designed the study and prepared the article.

Received January 28, 2014; revised March 27, 2014; accepted April 4, 2014; published April 22, 2014.

REFERENCES

Albrecht, C., Russinova, E., Hecht, V., Baaijens, E., and de Vries, S. (2005). The *Arabidopsis thaliana* SOMATIC EMBRYOGENESIS RECEPTOR-LIKE KINASES1 and 2 control male sporogenesis. Plant Cell **17:** 3337–3349.

Ariizumi, T., and Toriyama, K. (2011). Genetic regulation of sporopollenin synthesis and pollen exine development. Annu. Rev. Plant Biol. **62:** 437–460.

Aya, K., Ueguchi-Tanaka, M., Kondo, M., Hamada, K., Yano, K., Nishimura, M., and Matsuoka, M. (2009). Gibberellin modulates anther development in rice via the transcriptional regulation of GAMYB. Plant Cell **21:** 1453–1472.

Bai, M.Y., Shang, J.X., Oh, E., Fan, M., Bai, Y., Zentella, R., Sun, T.P., and Wang, Z.Y. (2012). Brassinosteroid, gibberellin and phytochrome impinge on a common transcription module in *Arabidopsis.* Nat. Cell Biol. **14:** 810–817.

Campuzano, S., and Modolell, J. (1992). Patterning of the *Drosophila* nervous system: the *achaete-scute* gene complex. Trends Genet. **8:** 202–208.

Canales, C., Bhatt, A.M., Scott, R., and Dickinson, H. (2002). EXS, a putative LRR receptor kinase, regulates male germline cell number and tapetal identity and promotes seed development in *Arabidopsis.* Curr. Biol. **12:** 1718–1727.

Chaubal, R., Anderson, J.R., Trimnell, M.R., Fox, T.W., Albertsen, M.C., and Bedinger, P. (2003). The transformation of anthers in the *msca1* mutant of maize. Planta **216:** 778–788.

Chen, L., Chu, H.W., Yuan, Z., Pan, A.H., Liang, W.Q., Huang, H., Shen, M.S., and Zhang, D.B. (2006). Isolation and genetic analysis for rice mutants treated with ^{60}Co γ-ray. J. Xiamen Univ. **45:** 81–85.

Chu, H.W., et al. (2005). Genetic analysis and mapping of the rice leafy-hull mutant *Oslh* (in Chinese). Zhi Wu Sheng Li Yu Fen Zi Sheng Wu Xue Xue Bao **31:** 594–598.

Colcombet, J., Boisson-Dernier, A., Ros-Palau, R., Vera, C.E., and Schroeder, J.I. (2005). *Arabidopsis* SOMATIC EMBRYOGENESIS RECEPTOR KINASES1 and 2 are essential for tapetum development and microspore maturation. Plant Cell **17:** 3350–3361.

Feng, B., Lu, D., Ma, X., Peng, Y., Sun, Y., Ning, G., and Ma, H. (2012). Regulation of the *Arabidopsis* anther transcriptome by DYT1 for pollen development. Plant J. **72:** 612–624.

Feng, X., Zilberman, D., and Dickinson, H. (2013). A conversation across generations: soma-germ cell crosstalk in plants. Dev. Cell **24:** 215–225.

Firulli, B.A., Hadzic, D.B., McDaid, J.R., and Firulli, A.B. (2000). The basic helix-loop-helix transcription factors dHAND and eHAND exhibit dimerization characteristics that suggest complex regulation of function. J. Biol. Chem. **275:** 33567–33573.

Hachez, C., Ohashi-Ito, K., Dong, J., and Bergmann, D.C. (2011). Differentiation of *Arabidopsis* guard cells: analysis of the networks incorporating the basic helix-loop-helix transcription factor, FAMA. Plant Physiol. **155:** 1458–1472.

Hird, D.L., Worrall, D., Hodge, R., Smartt, S., Paul, W., and Scott, R. (1993). The anther-specific protein encoded by the *Brassica napus* and *Arabidopsis thaliana A6* gene displays similarity to beta-1,3-glucanases. Plant J. **4:** 1023–1033.

Hong, L., Tang, D., Shen, Y., Hu, Q., Wang, K., Li, M., Lu, T., and Cheng, Z. (2012b). MIL2 (MICROSPORELESS2) regulates early cell differentiation in the rice anther. New Phytol. **196:** 402–413.

Hong, L., Tang, D., Zhu, K., Wang, K., Li, M., and Cheng, Z. (2012a). Somatic and reproductive cell development in rice anther is regulated by a putative glutaredoxin. Plant Cell **24:** 577–588.

Hord, C.L., Chen, C., Deyoung, B.J., Clark, S.E., and Ma, H. (2006). The BAM1/BAM2 receptor-like kinases are important regulators of *Arabidopsis* early anther development. Plant Cell **18:** 1667–1680.

Jung, K.H., Han, M.J., Lee, Y.S., Kim, Y.W., Hwang, I., Kim, M.J., Kim, Y.K., Nahm, B.H., and An, G. (2005). Rice *Undeveloped Tapetum1* is a major regulator of early tapetum development. Plant Cell **17:** 2705–2722.

Kaneko, M., Inukai, Y., Ueguchi-Tanaka, M., Itoh, H., Izawa, T., Kobayashi, Y., Hattori, T., Miyao, A., Hirochika, H., Ashikari, M., and Matsuoka, M. (2004). Loss-of-function mutations of the rice *GAMYB* gene impair alpha-amylase expression in aleurone and flower development. Plant Cell **16:** 33–44.

Kelliher, T., and Walbot, V. (2011). Emergence and patterning of the five cell types of the *Zea mays* anther locule. Dev. Biol. **350:** 32–49.

Lampard, G.R. (2009). The missing link?: *Arabidopsis* SPCH is a MAPK specificity factor that controls entry into the stomatal lineage. Plant Signal. Behav. **4:** 425–427.

Lee, S., Jung, K.H., An, G., and Chung, Y.Y. (2004). Isolation and characterization of a rice cysteine protease gene, *OsCP1*, using T-DNA gene-trap system. Plant Mol. Biol. **54:** 755–765.

Li, H., Pinot, F., Sauveplane, V., Werck-Reichhart, D., Diehl, P., Schreiber, L., Franke, R., Zhang, P., Chen, L., Gao, Y., Liang, W., and Zhang, D. (2010). Cytochrome P450 family member CYP704B2 catalyzes the omega-hydroxylation of fatty acids and is required for anther cutin biosynthesis and pollen exine formation in rice. Plant Cell **22:** 173–190.

Li, H., Yuan, Z., Vizcay-Barrena, G., Yang, C., Liang, W., Zong, J., Wilson, Z.A., and Zhang, D. (2011). *PERSISTENT TAPETAL CELL1* encodes a PHD-finger protein that is required for tapetal cell death and pollen development in rice. Plant Physiol. **156:** 615–630.

Li, N., et al. (2006). The rice *tapetum degeneration retardation* gene is required for tapetum degradation and anther development. Plant Cell **18:** 2999–3014.

Li, S., Gutsche, N., and Zachgo, S. (2011). The ROXY1 C-terminal L**LL motif is essential for the interaction with TGA transcription factors. Plant Physiol. **157:** 2056–2068.

Li, S.F., Iacuone, S., and Parish, R.W. (2007). Suppression and restoration of male fertility using a transcription factor. Plant Biotechnol. J. **5:** 297–312.

Li, X., Gao, X., Wei, Y., Deng, L., Ouyang, Y., Chen, G., Li, X., Zhang, Q., and Wu, C. (2011). Rice APOPTOSIS INHIBITOR5 coupled with two DEAD-box adenosine 5′-triphosphate-dependent RNA helicases regulates tapetum degeneration. Plant Cell **23:** 1416–1434.

Li, X., et al. (2006). Genome-wide analysis of basic/helix-loop-helix transcription factor family in rice and *Arabidopsis.* Plant Physiol. **141:** 1167–1184.

Liu, X., Huang, J., Parameswaran, S., Ito, T., Seubert, B., Auer, M., Rymaszewski, A., Jia, G., Owen, H.A., and Zhao, D. (2009). The *SPOROCYTELESS/NOZZLE* gene is involved in controlling stamen identity in *Arabidopsis.* Plant Physiol. **151:** 1401–1411.

Liu, Z., Bao, W., Liang, W., Yin, J., and Zhang, D. (2010). Identification of *gamyb-4* and analysis of the regulatory role of *GAMYB* in rice anther development. J. Integr. Plant Biol. **52:** 670–678.

Ma, H. (2005). Molecular genetic analyses of microsporogenesis and microgametogenesis in flowering plants. Annu. Rev. Plant Biol. **56:** 393–434.

Ma, X., Feng, B., and Ma, H. (2012). AMS-dependent and independent regulation of anther transcriptome and comparison with those affected by other *Arabidopsis* anther genes. BMC Plant Biol. **12:** 23.

MacAlister, C.A., Ohashi-Ito, K., and Bergmann, D.C. (2007). Transcription factor control of asymmetric cell divisions that establish the stomatal lineage. Nature **445:** 537–540.

Millar, A.A., and Gubler, F. (2005). The *Arabidopsis GAMYB-like* genes, *MYB33* and *MYB65*, are microRNA-regulated genes that redundantly facilitate anther development. Plant Cell **17:** 705–721.

Mizuno, S., Osakabe, Y., Maruyama, K., Ito, T., Osakabe, K., Sato, T., Shinozaki, K., and Yamaguchi-Shinozaki, K. (2007). Receptor-like protein kinase 2 (RPK 2) is a novel factor controlling anther development in *Arabidopsis thaliana.* Plant J. **50:** 751–766.

Murmu, J., Bush, M.J., DeLong, C., Li, S., Xu, M., Khan, M., Malcolmson, C., Fobert, P.R., Zachgo, S., and Hepworth, S.R. (2010). *Arabidopsis* basic leucine-zipper transcription factors TGA9 and TGA10 interact with floral glutaredoxins ROXY1 and ROXY2 and are redundantly required for anther development. Plant Physiol. **154:** 1492–1504.

Niu, N., Liang, W., Yang, X., Jin, W., Wilson, Z.A., Hu, J., and Zhang, D. (2013). EAT1 promotes tapetal cell death by regulating aspartic proteases during male reproductive development in rice. Nat. Commun. **4:** 1445.

Nonomura, K., Miyoshi, K., Eiguchi, M., Suzuki, T., Miyao, A., Hirochika, H., and Kurata, N. (2003). The *MSP1* gene is necessary to restrict the number of cells entering into male and female sporogenesis and to initiate anther wall formation in rice. Plant Cell **15:** 1728–1739.

Ohashi-Ito, K., and Bergmann, D.C. (2006). *Arabidopsis* FAMA controls the final proliferation/differentiation switch during stomatal development. Plant Cell **18:** 2493–2505.

Olson, E.N. (1990). MyoD family: a paradigm for development? Genes Dev. **4:** 1454–1461.

Paul, W., Hodge, R., Smartt, S., Draper, J., and Scott, R. (1992). The isolation and characterisation of the tapetum-specific *Arabidopsis thaliana A9* gene. Plant Mol. Biol. **19:** 611–622.

Phan, H.A., Iacuone, S., Li, S.F., and Parish, R.W. (2011). The MYB80 transcription factor is required for pollen development and the regulation of tapetal programmed cell death in *Arabidopsis thaliana.* Plant Cell **23:** 2209–2224.

Pillitteri, L.J., and Torii, K.U. (2012). Mechanisms of stomatal development. Annu. Rev. Plant Biol. **63:** 591–614.

Pillitteri, L.J., Sloan, D.B., Bogenschutz, N.L., and Torii, K.U. (2007). Termination of asymmetric cell division and differentiation of stomata. Nature **445:** 501–505.

Schiefthaler, U., Balasubramanian, S., Sieber, P., Chevalier, D., Wisman, E., and Schneitz, K. (1999). Molecular analysis of *NOZZLE*, a gene involved in pattern formation and early sporogenesis during sex organ development in *Arabidopsis thaliana.* Proc. Natl. Acad. Sci. USA **96:** 11664–11669.

Shi, J., et al. (2011). *Defective pollen wall* is required for anther and microspore development in rice and encodes a fatty acyl carrier protein reductase. Plant Cell **23:** 2225–2246.

Shi, Y., Zhao, S., and Yao, J. (2009). Premature tapetum degeneration: a major cause of abortive pollen development in photoperiod sensitive genic male sterility in rice. J. Integr. Plant Biol. **51:** 774–781.

Sorensen, A.M., Kröber, S., Unte, U.S., Huijser, P., Dekker, K., and Saedler, H. (2003). The *Arabidopsis ABORTED MICROSPORES* (*AMS*) gene encodes a MYC class transcription factor. Plant J. **33:** 413–423.

Tan, H., Liang, W., Hu, J., and Zhang, D. (2012). *MTR1* encodes a secretory fasciclin glycoprotein required for male reproductive development in rice. Dev. Cell **22:** 1127–1137.

Triviño, M., Martín-Trillo, M., Ballesteros, I., Delgado, D., de Marcos, A., Desvoyes, B., Gutiérrez, C., Mena, M., and Fenoll, C. (2013). Timely expression of the *Arabidopsis* stoma-fate master regulator MUTE is required for specification of other epidermal cell types. Plant J. **75:** 808–822.

Tsuji, H., Aya, K., Ueguchi-Tanaka, M., Shimada, Y., Nakazono, M., Watanabe, R., Nishizawa, N.K., Gomi, K., Shimada, A., Kitano, H., Ashikari, M., and Matsuoka, M. (2006). GAMYB controls different sets of genes and is differentially regulated by microRNA in aleurone cells and anthers. Plant J. **47:** 427–444.

Walbot, V., and Evans, M.M. (2003). Unique features of the plant life cycle and their consequences. Nat. Rev. Genet. **4:** 369–379.

Wan, L., Zha, W., Cheng, X., Liu, C., Lv, L., Liu, C., Wang, Z., Du, B., Chen, R., Zhu, L., and He, G. (2011). A rice β-1,3-glucanase gene *Osg1* is required for callose degradation in pollen development. Planta **233:** 309–323.

Wang, C.J., Nan, G.L., Kelliher, T., Timofejeva, L., Vernoud, V., Golubovskaya, I.N., Harper, L., Egger, R., Walbot, V., and Cande, W.Z. (2012). Maize *multiple archesporial cells 1* (*mac1*), an ortholog of rice *TDL1A*, modulates cell proliferation and identity in early anther development. Development **139:** 2594–2603.

Wang, M., Wang, K., Tang, D., Wei, C., Li, M., Shen, Y., Chi, Z., Gu, M., and Cheng, Z. (2010). The central element protein ZEP1 of the synaptonemal complex regulates the number of crossovers during meiosis in rice. Plant Cell **22:** 417–430.

Weintraub, H. (1993). The MyoD family and myogenesis: redundancy, networks, and thresholds. Cell **75:** 1241–1244.

Weintraub, H., et al. (1991). The *myoD* gene family: nodal point during specification of the muscle cell lineage. Science **251:** 761–766.

Wilson, Z.A., and Zhang, D.B. (2009). From *Arabidopsis* to rice: pathways in pollen development. J. Exp. Bot. **60:** 1479–1492.

Xu, J., Yang, C., Yuan, Z., Zhang, D., Gondwe, M.Y., Ding, Z., Liang, W., Zhang, D., and Wilson, Z.A. (2010). The *ABORTED MICROSPORES* regulatory network is required for postmeiotic male reproductive development in *Arabidopsis thaliana.* Plant Cell **22:** 91–107.

Yang, S.L., Jiang, L., Puah, C.S., Xie, L.F., Zhang, X.Q., Chen, L.Q., Yang, W.C., and Ye, D. (2005). Overexpression of *TAPETUM DETERMINANT1* alters the cell fates in the *Arabidopsis* carpel and tapetum via genetic interaction with *excess microsporocytes1*/*extra sporogenous cells.* Plant Physiol. **139:** 186–191.

Yang, S.L., Xie, L.F., Mao, H.Z., Puah, C.S., Yang, W.C., Jiang, L., Sundaresan, V., and Ye, D. (2003). *Tapetum determinant1* is required for cell specialization in the *Arabidopsis* anther. Plant Cell **15:** 2792–2804.

Yang, W.C., Ye, D., Xu, J., and Sundaresan, V. (1999). The *SPOROCYTELESS* gene of *Arabidopsis* is required for initiation of sporogenesis and encodes a novel nuclear protein. Genes Dev. **13:** 2108–2117.

Zhang, D., and Yang, L. (2014). Specification of tapetum and microsporocyte cells within the anther. Curr. Opin. Plant Biol. **17:** 49–55.

Zhang, D., Luo, X., and Zhu, L. (2011). Cytological analysis and genetic control of rice anther development. J. Genet. Genomics **38:** 379–390.

Zhang, D., Liang, W., Yin, C., Zong, J., Gu, F., and Zhang, D. (2010). *OsC6*, encoding a lipid transfer protein, is required for postmeiotic anther development in rice. Plant Physiol. **154:** 149–162.

Zhang, D.S., Liang, W.Q., Yuan, Z., Li, N., Shi, J., Wang, J., Liu, Y.M., Yu, W.J., and Zhang, D.B. (2008). Tapetum degeneration retardation is critical for aliphatic metabolism and gene regulation during rice pollen development. Mol. Plant **1:** 599–610.

Zhang, W., Sun, Y., Timofejeva, L., Chen, C., Grossniklaus, U., and Ma, H. (2006). Regulation of *Arabidopsis* tapetum development and function by *DYSFUNCTIONAL TAPETUM1* (*DYT1*) encoding a putative bHLH transcription factor. Development **133:** 3085–3095.

Zhang, Z., et al. (2007). Transcription factor AtMYB103 is required for anther development by regulating tapetum development, callose dissolution and exine formation in Arabidopsis. Plant J. **52:** 528–538.

Zhao, D.Z., Wang, G.F., Speal, B., and Ma, H. (2002). The *excess microsporocytes1* gene encodes a putative leucine-rich repeat receptor protein kinase that controls somatic and reproductive cell fates in the *Arabidopsis* anther. Genes Dev. **16:** 2021–2031.

Zhao, X., de Palma, J., Oane, R., Gamuyao, R., Luo, M., Chaudhury, A., Hervé, P., Xue, Q., and Bennett, J. (2008). OsTDL1A binds to the LRR domain of rice receptor kinase MSP1, and is required to limit sporocyte numbers. Plant J. **54:** 375–387.